WAKE INTERFERENCE ON THE FLOW AROUND AN OSCILLATING CIRCULAR CYLINDER IN GROUND EFFECT

Washington Humberto de Moura, whmoura@uninove.br
Engineering Department, UNINOVE, Sao Paulo, Brazil

Alex Mendonça Bimbato, alexbimbato@unifei.edu.br
Luiz Antonio Alcântara Pereira, luizantp@unifei.edu.br
Institute of Mechanical Engineering, Federal University of Itajuba, Itajuba, Minas Gerais, Brazil, CP 50

Miguel Hiroo Hirata, hirata@fat.uerj.br
State University of Rio de Janeiro, FAT-UERJ, Resende, Rio de Janeiro, Brazil

Abstract. *The wake interference of a transversely oscillating circular cylinder placed near and parallel to a ground is investigated by numerical calculations using vortex particles. To investigate the wake interference, two plane wall configurations are considered: with and without the influence of the ground boundary layer. When the plane wall is running at the same speed as the freestream no boundary layer develops to interfere with the cylinder. The amplitude of the oscillatory motion is considered to be small compared to the cylinder diameter, therefore, to the first approximation, one is allowed to transfer the body boundary condition from the actual position to a mean position of the body surface. Our results for aerodynamic loads and Strouhal number are presented and discussed.*

Keywords*: heaving cylinder, fixed ground, moving ground, aerodynamic loads, vortex method*

1. INTRODUCTION

Understanding oscillation of bluff bodies relative to an incident fluid flow is of great importance in the design of a variety of engineering problems. In particular, oscillatory motions of small amplitude are important in the analysis of an immerse vibrating body and special care should be taken in the lock-in condition. The problem described can be compared with many engineering situations where it is possible verify changes in the velocity field around a body thus a surface localized near the neighborhood. An automobile near the ground and an aircraft landing or taking off are examples of this phenomenon.

For a better and easy understanding of the physics, therefore, it is reasonable to focus our attention on the flow around bodies of simple geometry. One of the most investigated vortex-induced vibrations is that the flow around an oscillating circular cylinder; it is known that the vortex shedding frequency f had been found to lock-in to the forcing frequency f_b when f_b is close to the free vortex shedding frequency f_{so} in the transverse oscillating case. But, the in-line vibration lock-in takes place at a number of multiple ratios of f_b/f_{so}, especially, at f_b/f_{so} =2.0, where the lift and drag forces increase greatly. Comprehensive reviews can be found in Koopman (1967), Sarpkaya (1979), Bearman (1984), Blevins (1990), Griffin and Hall (1991), Williamson and Govardhan (2004) and Hirata *et al.* (2008).

On the other hand, the fluid flow around a fixed circular cylinder close to a plane wall is governed not only by the Reynolds number but also by the gap between the cylinder and the ground, h, characterized by the gap ratio h/d (d is cylinder diameter). The fundamental effects of gap ratio have been observed e.g. by Taneda (1965), Roshko *et al.* (1975), Bearman and Zdravkovich (1978), Angrilli *et al.* (1982), Grass *et al.* (1984), Zdravkovich (1985a), Price *et al.* (2002) and Lin *et al.* (2005).

However, the influence of the boundary layer formed on the ground is much more complicated and is still unclear despite several intensive studies reported so far. Roshko *et al.* (1975) measured the time-averaged drag and lift coefficients, C_D and C_L, for a circular cylinder placed near a fixed wall in a wind tunnel at $Re=2.0\times10^4$, which lies in the upper-subcritical flow regime, and showed that the C_D rapidly decreased and C_L increased as the cylinder came close to the wall. Zdravkovich (1985b) observed, in his force measurements performed at $4.8\times10^4 < Re < 3.0\times10^5$, that the rapid decrease in drag occurred as the gap was reduced to less than the thickness of the boundary layer δ/d on the ground, and concluded that the variation of C_D was dominated by h/δ rather than by the conventional gap ratio h/d. He also noted that the C_L could be significantly affected by the state of the boundary layer, although it was insensitive to the thickness of the boundary layer.

Zdravkovich (2003) reported the drag behavior for cylinder placed near a moving ground running at the same speed as the freestream for higher Reynolds number of 2.5×10^5, which lies within the critical flow regime rather than the subcritical flow regime. The experiment by Zdravkovich (2003) showed contrast to all the above studies. First, practically no boundary layer on the ground. Second, the decrease in drag due the decrease in h/d did not occur in his measurements. The differences encountered were attributed to the non-existence of the wall boundary layer or the higher Reynolds number. Nishino (2007) presented experimental results of a circular cylinder with an aspect ratio of 8.33, with and without end-plates, placed near and parallel to a moving ground, on which substantially no boundary

layer developed to interface with the cylinder. Measurements were carried out at two upper-subcritical Reynolds numbers of 0.4 and 1.0×10^5. The results produced new insights into the physics of ground effect, and could serve as a database for both experimental and computational studies on the ground effect in the future. According to Nishino (2007) experiments, for the cylinder with end-plates, on which the oil flow patterns were observed to be essentially two-dimensional, the drag rapidly decrease as h/d decrease to less than 1.0 but became constant for h/d of less than 0.35, unlike that usually observed near a fixed ground (as will be plotted later in "Fig. 2a").

Vortex method offer a number of advantages over the more traditional Eulerian schemes for the numerical analysis of the external flow that develops in a large domain; the main reasons are [Sarpkaya (1989), Lewis (1999), Kamemoto (2004), Alcântara Pereira *et al.* (2004) and Hirata *et al.* (2008)]: (i) as a fully mesh-less scheme, no grid is necessary; (ii) the computational efforts are directed only to the regions with non-zero vorticity and not to all the domain points as is done in the Eulerian formulations; (iii) the far away downstream boundary condition is taken care automatically which is relevant for the simulation of the flow around a bluff body (or an oscillating body) that has a wide viscous wake.

Moura (2007) studied numerically the two-dimensional, incompressible unsteady flow around a circular cylinder near a fixed ground using the vortex method. The body was animate by a forced frequency. He investigated the influence of the heave movement with small amplitude on the aerodynamic loads of the cylinder placed near a fixed ground.

In a recent work, Bimbato (2008) used the vortex method to study the aerodynamic loads acting on a circular cylinder surface placed near a ground running at the same speed as the incident flow in which the vorticity was generate only from the body surface. The results agree with that presented by Nishino (2007) when the end-plates were used.

In this paper, the vortex method is used to simulate the viscous flow around an oscillating circular cylinder in ground effect. Two plane wall configurations are considered: fixed ground and moving ground. In all the numerical experiments the Reynolds number is kept in high value, $Re=1.0x10^5$. Even with such a high Reynolds number value, no attempt for turbulence modeling were made once these aspects have a strong three-dimensional component; see Alcântara Pereira *et al.* (2004).

2. PROBLEM FORMULATION AND VORTEX METHOD

Consider the incompressible flow of a Newtonian fluid in a large two-dimensional domain around a circular cylinder which moves with constant velocity U in ground effect. An oscillatory motion with finite amplitude A and constant angular velocity λ is added to body as shown in Fig. 1. In this figure the (x, o, y) is the inertial frame of reference and the (ξ, o, η) is the coordinate system fixed to the cylinder; the inertial frame oscillates around the x-axis as $y_0=A\cos(\lambda t)$, where $\lambda=2\pi f_b$ and f_b is the body oscillation frequency.

The boundary S of the fluid domain Ω is $S = S_1 \cup S_2 \cup S_3$; being S_3 the far away boundary, which can be viewed as $r = \sqrt{x^2 + y^2} \to \infty$, and S_1 the body surface and S_2 the fixed ground plane surface.

The vorticity that develops in the body boundary layer is carried out downstream into the viscous wake. Due to the no-slip condition, a shear flow is set on the fixed ground. As consequence, there is vorticity generated on the fixed ground and the body wake will be influenced by the presence of the plane wall wake, as can be seen in Fig. 1. A ground running at the same speed as the freestream, however, does not allow the development of boundary layer.

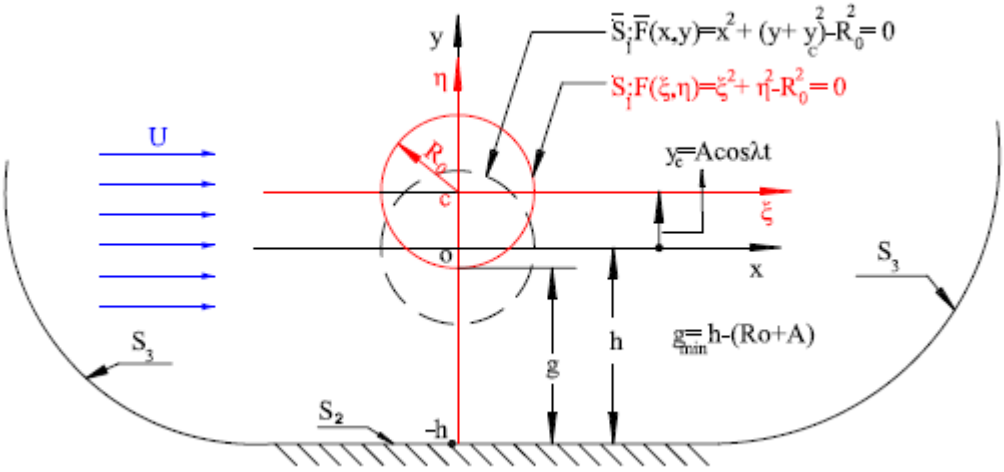

Figure 1. Definitions.

When the body is represented by a circular cylinder:

$$F_1(\xi,\eta) = \xi^2 + \eta^2 - R_0^2 = 0 \tag{1}$$

$$x_C = \xi$$

$$y_C = y_0 + \eta, \tag{2}$$

$$S_1 : F_1(x,y) = x_c^2 + (y_c - y_0)^2 - R_0^2 = 0 \tag{3}$$

The mean position of circular cylinder surface is defined as

$$\overline{S}_1 : \overline{F}_1(x,y) = \overline{x}_C{}^2 + \overline{y}_c{}^2 - R_0{}^2 = 0 \tag{4}$$

For symmetric body

$$F_1(x,y) = \eta_c \pm \varphi(\xi) = 0 \tag{5}$$

where $\varphi(\xi)$ indicate the body thickness.

The ground plane surface S_2 is defined as

$$y = -h, -\infty < x < \infty \tag{6}$$

The viscous and incompressible flow is governed by the continuity and the Navier-Stokes equations, which can be written in the form

$$\nabla \cdot \mathbf{u} = 0 \tag{7}$$

$$\frac{\partial \mathbf{u}}{\partial t} + \mathbf{u} \cdot \nabla \mathbf{u} = -\nabla p + \frac{1}{Re} \nabla^2 \mathbf{u} \tag{8}$$

where $\mathbf{u} \equiv (u, v)$ is the velocity vector. As can be seen the equations are no-dimensionalized in terms of U and d (cylinder diameter: $d = 2R$). The Reynolds number is defined by

$$Re = \frac{Ud}{\upsilon} \tag{8a}$$

where υ is the fluid kinematics viscosity coefficient; the dimensionless time is d / U.

On the body and ground plane surfaces the adherence condition has to be satisfied. This condition is better specified in terms of the normal and tangential components as

$(\mathbf{u} \cdot \mathbf{n}) = (\mathbf{v} \cdot \mathbf{n})$ on S_1 and S_2, the impenetrability condition (9a)

$(\mathbf{u} \cdot \boldsymbol{\tau}) = (\mathbf{v} \cdot \boldsymbol{\tau})$ on S_1 and S_2, the no-slip condition for fixed ground case (9b)

$(\mathbf{u} \cdot \boldsymbol{\tau}) = (\mathbf{v} \cdot \boldsymbol{\tau})$ on S_1, the no-slip condition for moving ground case (9c)

Here $\mathbf{n}$ and $\boldsymbol{\tau}$ are unit normal and tangential vectors and v is the surfaces velocity: S_1 and S_2. It is worth to mention the necessity of imposing the impermeability condition on the surface of the moving ground.

Far from the surfaces S_1 and S_2 one assumes that the perturbation due to the oscillating body fades away, that is

$$|\mathbf{u}| \to 1 \text{ at } S_3 \tag{10}$$

Is considered an small amplitude around the axis x, therefore

$$\frac{A}{2R} = O(\varepsilon), \text{ where } \varepsilon \to 0 \text{ and } \lambda = O(1) \tag{11}$$

Thus, the boundary conditions on S_1 are written directly in the inertial frame of reference as

$$u_n(x,y,t) \equiv \left[v_n(x,y,t)\right] \text{ on } S_1, \text{ the impenetrability condition} \tag{12a}$$

$$u_\tau(x,y,t) \equiv \left[v_\tau(x,y,t)\right] \text{ on } S_1, \text{ the no-slip condition} \tag{12b}$$

The transference of the boundary conditions on S_1 from actual position to the mean position is defined as

$$y_c = y_0 + \eta(x) \;\rightarrow\; \bar{y}_c = \eta(x) + O(y_0) \tag{13a}$$

$$u_n(x_c, y_c, t) = u_n\left(x_c, y_0 + \eta, t\right) = u_n\left(x_c, \eta(x_c), t\right) + y_0 \frac{\partial u_n\left(x_c, \eta(x_c), t\right)}{\partial y} + \cdots \tag{13b}$$

$$u_\tau(x_c, y_c, t) = u_\tau\left(x_c, y_0 + \eta, t\right) = u_\tau\left(x_c, \eta(x_c), t\right) + y_0 \frac{\partial u_\tau\left(x_c, \eta(x_c), t\right)}{\partial y} + \cdots \tag{13c}$$

The dynamics of the fluid motion, governed by the above boundary-value problem, can be alternatively studied by taking the curl of Eq. (8), obtaining the well-known 2-D vorticity transport equation

$$\frac{\partial \omega}{\partial t} + \mathbf{u}\cdot\nabla\omega = \frac{1}{Re}\nabla^2\omega \tag{14}$$

where ω is the only non-zero component of the vorticity vector $\boldsymbol{\omega} = \nabla\times\mathbf{u}$.

According to the convection-diffusion splitting algorithm (Chorin, 1973) it is assumed that in the same time increment the convection and the diffusion of the vorticity can be independently handled and are governed by

$$\frac{\partial \omega}{\partial t} + \mathbf{u}\cdot\nabla\omega = 0 \tag{15}$$

$$\frac{\partial \omega}{\partial t} = \frac{1}{Re}\nabla^2\omega \tag{16}$$

Once the vorticity field is modeled by a cloud of discrete vortices, the convection Eq. (15) is written in Lagrangian form as

$$\frac{d\mathbf{x}_j}{dt} = \mathbf{u}_j(\mathbf{x},t) \quad j = 1, NV \tag{15a}$$

where NV is the number of point vortices in the cloud and the velocity field $\mathbf{u}(\mathbf{x},t)$ can be split in three parts (Hirata *et al.*, 2008)

$$\mathbf{u}(\mathbf{x},t) = \mathbf{ui}(\mathbf{x},t) + \mathbf{ub}(\mathbf{x},t) + \mathbf{uv}(\mathbf{x},t) \tag{17}$$

The contribution of the incident flow is represented by $\mathbf{ui}(\mathbf{x},t)$. For an uniform oncoming flow its components take the form

$$ui_1 = 1 \text{ and } ui_2 = 0 \tag{18}$$

The body contributes with **ub**(**x**,t), which can be obtained, for example, using the Boundary Element Method.
The fluid velocity on the circular cylinder surface is written as

$$\mathbf{u}(\xi,\eta;t) = U\mathbf{i} - \dot{y}_0(t)\mathbf{j}\,;\ \text{with}\ \dot{y}_0(t) = \frac{d}{dt}\left[A\cos(\lambda t)\right] \tag{19}$$

As a consequence of the **j** component of the right hand side of the fluid velocity (in the above expression) one gets an additional singularities distribution on the body surface. Of course, the induced velocity due to this additional singularities distribution fades away from the body.

The velocity induced by the body, according to the Panels Method calculations (Katz and Plotkin, 1991), is indicated by [uc(ξ,η), vc(ξ,η)]; this is the velocity induced at the vortex (i), located at the point [x(t), y(t)], thus

$$uc^{(i)}(x,y;t) = uc(\xi,\eta;t) \tag{17a}$$

$$vc^{(i)}(x,y;t) = vc(\xi,\eta;t) \tag{17b}$$

where the following relations remains

$$x^{(i)}(t) = \xi \tag{18a}$$

$$y^{(i)}(t) = y_0(t) + \eta \tag{18b}$$

The process of vorticity generation is carried out from Eq. (9b), so as to satisfy the no-slip condition. According to the discussion above the Panels Method guaranties that the impermeability condition is satisfied in each straight-line element, or panel, at pivotal point. At each instant of the time 2M new vortices are created a small distance ε of the body and fixed ground plane surfaces, whose strengths are determined from Eq. (9b) applied at 2M point's right below the newly created vortices, along the radial direction. This procedure yields an algebraic system of 2M equations and 2M unknowns (the strengths of the vortices). When using moving ground, this procedure yields an algebraic system of M equations and M unknowns.

The vorticity field is discretized and represented by a cloud of discrete Lamb vortices, whose mathematical expression for the induced velocity of the k-th vortex with strength $\Delta\Gamma_k$ in the circumferential direction u_{θ_k} is (Mustto *et al.*, 1998)

$$u_{\theta_k} = \frac{\Delta\Gamma_k}{2\pi r}\left\{1 - \exp\left[-5.02572\left(-\frac{r}{\sigma_0}\right)^2\right]\right\} \tag{19}$$

where σ_0 is core radius of the Lamb vortex.

In this particular equation r is the radial distance between the vortex center and the point in the flow field where the induced velocity is calculated.

Each vortex particle distributed in the flow field is followed during numerical simulation according to the Euler first-order formula

$$z(t+\Delta t) = z(t) + u(t)\Delta t + \xi \tag{20}$$

in which z is the position of a particle, Δt is the time increment and ξ is the random walk displacement with a zero mean and a (2Δt/Re) variance. According to Lewis (1999), the random walk displacement is given by

$$\xi = \sqrt{4\beta\Delta t \ln\left(\frac{1}{P}\right)}\left[\cos(2\pi Q) + i\sin(2\pi Q)\right] \tag{21}$$

where $\beta = Re^{-1}$; P and Q are random numbers between 0.0 and 1.0.

The pressure calculation starts with the Bernoulli function, defined as

$$Y = p + \frac{u^2}{2},\ u = |\mathbf{u}| \tag{22}$$

In the present approach the following integral formulation (Shintani and Akamatsu, 1994) is defined

$$H\overline{Y_i} - \int_{S_1} \overline{Y} \nabla G_i \cdot \mathbf{e}_n dS = \iint_{\Omega} \nabla G_i \cdot (\mathbf{u} \times \omega) d\Omega - \frac{1}{Re} \int_{S_1} (\nabla G_i \times \omega) \cdot \mathbf{e}_n dS \tag{23}$$

where H is 1.0 inside the flow (at domain Ω) and is 0.5 on the boundaries S_1 and S_2. $G_i = (1/2\pi)\log R^{-1}$ is the fundamental solution of Laplace equation, R being the distance from i-th vortex element to the field point. It is worth to observe that this formulation is specially suited for a Lagrangian scheme because it utilizes the velocity and vorticity field defined at the position of the vortices in the cloud. Therefore it does not require any additional calculation at mesh points. Numerically, Eq. (23) is solved by mean of a set of simultaneous equations for pressure Y_i.

Details of the present numerical method are presented in Moura (2007) and Bimbato (2008).

3. RESULTS AND DISCUSSIONS

We preliminary investigate the flow around an isolated circular cylinder to analyze the consistence of the vortex code and to define some numerical parameters, as for example the number of panels used to define the cylinder surface. For this particular configuration, each cylinder and ground surface were represented by M=100 flat source panels with constant density. The simulation was performed up to 1000 time steps with magnitude Δt=0.05 (Mustto *et al*., 1998). During each time step the new vortex elements are shedding into the cloud through a displacement $\varepsilon=\sigma_0$=0.001d normal to the straight-line elements (panels); see Ricci (2002).

Table 1 shows that the numerical results agree very well with the experimental ones obtained by Blevins (1984), which have an uncertainty of about 10%. The results from Mustto *et al*. (1998) were obtained numerically using a slightly different vortex method from the present implementation. The agreement between the two numerical methods is very good for the Strouhal number, and both results are close to the experimental value. The present drag coefficient shows a higher value as compared to the experimental result. One should observe, that the three-dimensional effects are non-negligible for the Reynolds number used in the present simulation ($Re = 1.0\times10^5$). Therefore one can expect that a two-dimensional computation of such a flow must produce higher values for the drag coefficient. On the other hand, the Strouhal number is insensitive to these three-dimensional effects. The mean numerical lift coefficient, although very small, is not zero which is due to numerical approximations. The aerodynamic forces computations were evaluated between t=30 and t=50.

Table 1. Mean values of drag and lift coefficients and Strouhal number of an isolated circular cylinder

$Re = 1.0\times10^5$	$\overline{C_D}$	$\overline{C_L}$	$\overline{St}$
Blevins (1984)	1.20	-	0.19
Mustto *et al.* (1998)	1.22	-	0.22
Present Simulation	1.22	0.04	0.19

The Strouhal number is defined as

$$St = \frac{f\,d}{U} \tag{24}$$

where f is the detachment frequency of vortices of the lift coefficient. In general, one should observe that the lift coefficient oscillates with a dimensionless frequency (Strouhal number) that is one half the frequency of oscillation of the drag coefficient curve. More details of this preliminary study are discussed in Hirata *et al*. (2008).

In this paper, the body Strouhal number is defined as

$$St_b = \frac{f_b d}{U} \tag{25}$$

Figure 2 shows the behavior of drag and lift coefficients for circular cylinder at different values of the gap-ratio h/d and for different end conditions. The present numerical results are referred as "moving ground" and as "fixed ground" in Fig. 2. Columns 5 and 6 of Tab. 2 present our numerical values for drag coefficient of a fixed circular cylinder.

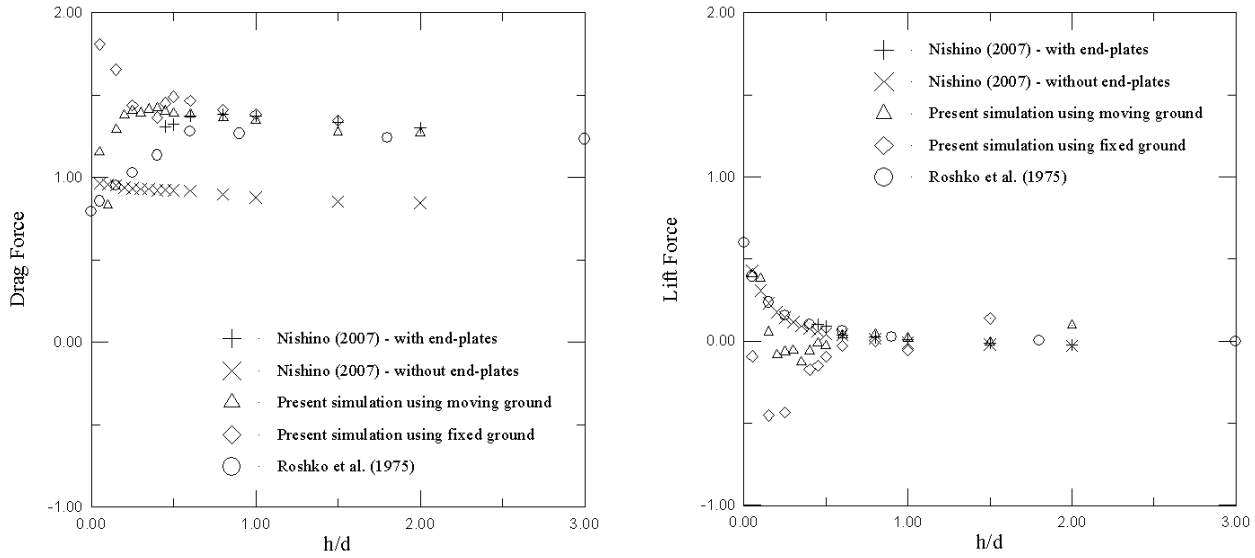

(a) Drag force (b) Lift force

Figure 2. Time-averaged drag and lift coefficients *vs.* gap ratio for different end conditions

Nishino (2007) investigated two flow configurations: one was essentially three-dimensional and another approximately two-dimensional; this second configuration was obtained by using end-plates on the cylinder extremity. It was shown that the drag coefficient on the 3-D flow increased slightly as the cylinder comes close to the ground, while the 2-D flow presented a higher drag coefficient.

Table 2. Summary of results for drag coefficient on the flow around fixed circular cylinder near a plane boundary

h/d	Nishino (2007) without end-plates	Nishino (2007) with end-plates	Roshko *et al.* (1975)	Present simulation: moving ground	Present simulation: fixed ground
0.00	-	-	0.795	-	-
0.05	0.965	-	0.857	1.154	1.809
0.10	0.958	-	-	0.832	-
0.15	0.952	-	0.954	1.293	1.656
0.20	0.939	-	-	1.376	-
0.25	0.933	-	1.029	1.406	1.440
0.30	0.930	-	-	1.393	-
0.35	0.931	-	-	1.415	-
0.40	0.922	-	1.136	1.421	1.365
0.45	0.926	1.311	-	1.403	1.453
0.50	0.924	1.323	-	1.391	1.491
0.60	0.920	1.373	1.281	1.383	1.466
0.80	0.899	1.385	-	1.362	1.410
0.90	-	-	1.266	-	-
1.00	0.881	1.375	-	1.346	1.385
1.50	0.854	1.337	-	1.277	1.346
2.00	0.845	1.304	-	1.269	-
3.00	-	-	1.234	-	-

The present simulations using moving ground reproduce the situation studied by Nishino (2007) with end-plates. One can see that the drag coefficient results of the 2-D numerical simulation agree well with the experimental results approximately 2-D from Nishino (2007). It is worth to observe that in this situation, due to the experimental difficulties, he was not able to perform the tests for small-gap regime (h/d<0.45).

As illustration, Tab. 3 present all the cases studied of vortex shedding from a transversely oscillating circular cylinder in ground effect for h/d=0.45. For these cases the effect of increase of the cylinder oscillation frequency is

investigated for a small amplitude A/d=0.05. We observe here that the lock-in feature is not identified; for instance, case V in Tab. 3 (fixed ground) had vortex-shedding frequency $\overline{S}_t$ =0.21, whereas the forcing frequency is S_{tb} =0.14.

Table 3. Circular cylinder: Results of C_L, C_D and Strouhal; h/d = 0.45, Re = 1.0x10^5 and A/d= 0. 05

Case		Fixed ground			Moving ground		
	S_{tb}	$\overline{C}_L$	$\overline{C}_D$	$\overline{S}_t$	$\overline{C}_L$	$\overline{C}_D$	$\overline{S}_t$
I	0.016	-0.114	1,437	0.19	-0.108	1.416	0.20
II	0.008	-0.087	1.409	0.20	-0.061	1.411	0.20
III	0.063	-0.125	1.399	0.20	-0.085	1.427	0.20
IV	0.110	-0.107	1.444	0.20	-0.055	1.319	0.21
V	0.140	-0.103	1.363	0.21	0.001	1.356	0.16

Figure 3 shows the time evolution of the aerodynamic forces acting on the oscillating circular cylinder surface placed near a fixed ground (see Fig. 3a) and near a moving ground (see Fig. 3b) using h/d = 0.45. In despite of proximity of the ground, the fluctuation of C_D has still twice the frequency that the C_L, this seems that it fluctuates once for each upper and lower shedding. The absolute values of the minimum and maximum of C_L curves are more representative in Fig. 3(b). When the ground is fixed, one can observe that the C_L curve has higher absolute value of the maximum than the absolute value of the maximum of the moving ground C_L curve case.

In the Fig. 3 are defined instants A, B, C, and D. At instant represented by the point A in Fig. 3a and Fig. 3b, one can identified a clockwise vortex structure detaching from the upper surface, see Fig. 4a and Fig. 4b. A low pressure zone on the upper side of the cylinder surface is developed, which explains the maximum C_L value (Moura, 2007).

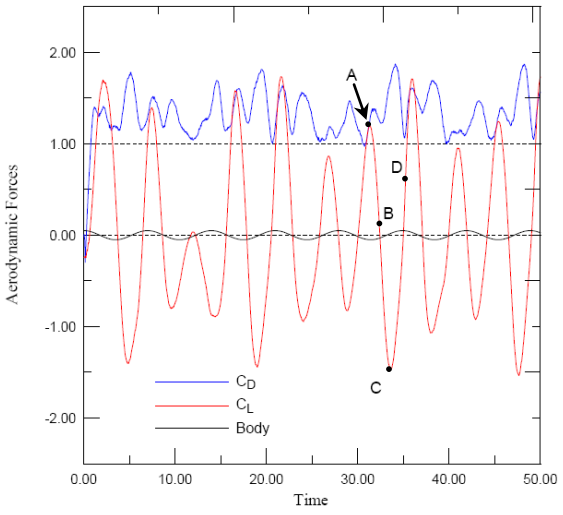

(a) moving ground

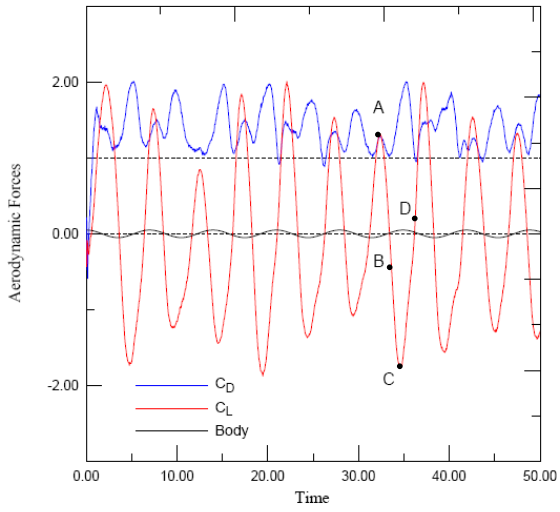

(b) fixed ground

Figure 3. Time history of drag and lift coefficients; h/d = 0.45, Re = 1.0x10^5, S_{tb} = 0.14 and A/d= 0. 05

As shown in Fig. 5 and Fig. 6, at the same instant represented by the point A, one can identified a low pressure zone on the upper side of the fixed cylinder surface, which explains the maximum C_L value again; as proceeds, at this moment a clockwise vortex structure is detaching from the upper surface; see Fig. 5a and Fig. 5b.

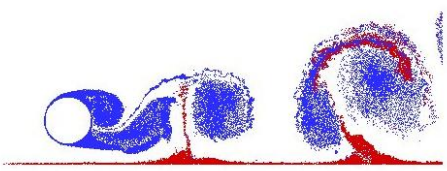

(a) fixed ground (S_{tb} =0.14 and A/d= 0. 05)

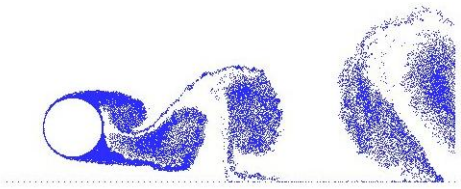

(b) moving ground (S_{tb} =0.14 and A/d= 0. 05)

Figure 4. Position of the wake vortices at an instant represented by point A, Re=1.0x10^5 and h/d=0.45

(a) fixed ground (S_{tb} =0.0 and A/d= 0. 0) (b) moving ground (S_{tb} =0.0 and A/d= 0. 0)

Figure 5. Near field velocity distribution at an instant represented by point A, Re=1.0x10^5 and h/d=0.45

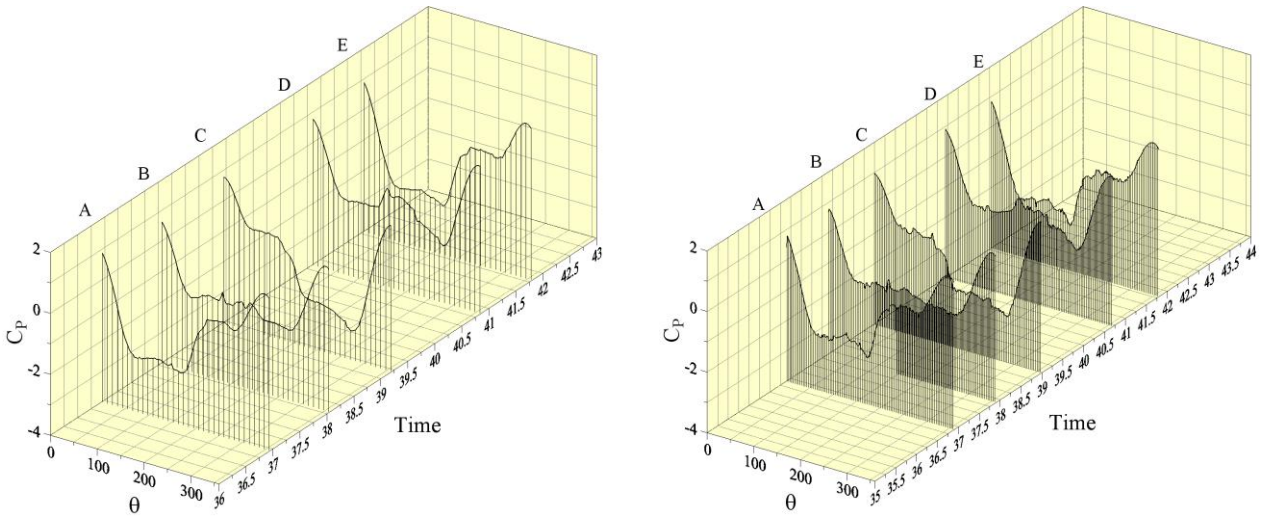

(a) fixed ground (S_{tb} =0.0 and A/d= 0. 0) (b) moving ground (S_{tb} =0.0 and A/d= 0. 0)

Figure 6. Instantaneous pressure distribution for the fixed circular cylinder in ground effect, Re=1.0x10^5 and h/d=0.45

4. CONCLUSIONS

Our results are able to predict the main features of the flow around an oscillating body (although with a simple geometrical shape) in ground effect. When using fixed ground and forcing frequency S_{tb} =0.0, the absolute value of the maximum of the C_D curve is bigger than the absolute value of the maximum of the moving ground C_D curve; the wake interference is the one responsible for a "great" maximum value of the C_D curve; see Bimbato (2008). In the present study, the wake interference was influenced by oscillatory motion. Our result for the oscillating circular cylinder case in ground effect no revealed estimative of the lock-in regime, and it needs further investigation for two cylinder configuration considered here. The experience gained with the present work allows us to analyze complex situations where relative motions between bodies are present. These extend the applicability of the vortex method code. Further analyses are necessary to understand the aerodynamic loads and vortex shedding behavior when the body is brought close to a plane wall. Future work will investigate the mechanisms of the heat transport from an oscillating heated cylinder in ground effect using two plane wall configurations (Recicar *et al.*, 2008).

5. ACKNOWLEDGEMENTS

We are pleased to acknowledge the support of this research by the CNPq (Brazilian Research Agency) Proc. 470420/2008-1, FAPERJ (Research Foundation of the State of Rio de Janeiro) Proc. E-26/112/013/2008 and FAPEMIG (Research Foundation of the State of Minas Gerais) Proc. TEC APQ-01074-08. The authors wish to thank Dr. Takafumi Nishino of the University of Southampton for send us comments about his experiments.

6. REFERENCES

Alcântara Pereira, L.A., Hirata, M.H. and Manzanares Filho, N., 2004, "Wake and Aerodynamics Loads in Multiple Bodies - Application to Turbomachinery Blade Rows", J. Wind Eng. Ind. Aerodyn., 92, pp. 477-491.

Angrilli, F, Bergamaschi, S. and Cossalter, V., 1982, "Investigation of Wall Induced Modifications to Vortex Shedding from a Circular Cylinder", Transactions of the ASME: Journal of Fluids Engineering, Vol. 104, pp. 518-522.

Bearman, P.W., 1984, "Vortex Shedding from Oscillating Bluff Bodies", Annu. Rev. Fluid Mech., 16:195-222.

Bearman, P.W. and Zdravkovich, M.M., 1978, "Flow around a Circular Cylinder near a Plane Boundary", Journal of Fluid Mechanics, Vol. 89, pp. 33-47.

Bimbato, A. M., 2008, Analysis of Moving Ground Effects on the Aerodynamic Loads of a Body, M.Sc. Dissertation, IEM/UNIFEI, (In Portuguese).

Blevins, R.D., 1990, "Flow Induced Vibrations", New York, Van Nostrand Reinhold.

Blevins, R. D., 1984, Applied Fluid Dynamics Handbook, Van Nostrand Reinhold, Co.

Chorin, A.J., 1973, "Numerical Study of Slightly Viscous Flow", Journal of Fluid Mechanics, Vol. 57, pp. 785-796.

Grass, A.J., Raven, P.W.J., Stuart, R.J. and Bray, J.A., 1984, "Influence of Boundary Layer Velocity Gradientes and Bed Proximity on Vortex Shedding from Free Spanning Pipelines", Transactions of the ASME: Journal of Energy Resources Technology, Vol. 106, pp. 70-78.

Griffin, O.M. and Hall, M.S., 1991, "Review-Vortex Shedding Lock-On and Flow Control in Bluff Body Wakes", Journal of Fluids Engineering, Vol. 113, pp. 526-537.

Hirata, M. H., Alcântara Pereira, L. A., Recicar, J. N., Moura, W. H., 2008, "High Reynolds Number Oscillations of a Circular Cylinder", J. of the Braz. Soc. Of Mech. Sci. & Eng., Vol. XXX, No. 4, pp. 300-308.

Kamemoto, K., 2004, "On Contribution of Advanced Vortex Element Methods Toward Virtual Reality of Unsteady Vortical Flows in the New Generation of CFD", Proceedings of the 10th Brazilian Congress of Thermal Sciences and Engineering-ENCIT 2004, Rio de Janeiro, Brazil, Nov. 29 - Dec. 03, Invited Lecture-CIT04-IL04.

Katz, J. and Plotkin, A., 1991, "Low Speed Aerodynamics: From Wing Theory to Panel Methods". McGraw Hill, Inc.

Koopman, G.H., 1967, "The Vortex Wakes of Vibrating Cylinders at Low Reynolds Numbers", Journal of Fluid Mechanics, Vol. 28, pp. 501-518.

Lewis, R.I., 1999, "Vortex Element Methods, the Most Natural Approach to Flow Simulation - A Review of Methodology with Applications", Proceedings of 1st Int. Conference on Vortex Methods, Kobe, Nov. 4-5, pp. 1-15.

Lin, C., Lin, W.J. and Lin, S.S., 2005, "Flow Characteristics around a Circular Cylinder near a Plane Boundary", Proceedings of the Sixteenth International Symposium on Transport Phenomena (ISTP-16), 29 August – 1 September, Prague, Czech Republic, (CD-ROOM).

Moura, W. H., 2007, Analysis of the Flow around an Oscillating Circular Cylinder in the Vicinity of a Ground Plane, M.Sc. Dissertation, IEM/UNIFEI (in Portuguese).

Mustto, A. A., Hirata, M. H. and Bodstein, G. C. R., 1998, "Discrete Vortex Method Simulation of the Flow around a Circular Cylinder with and without Rotation", A.I.A.A. Paper 98-2409, Proceedings of the 16th A.I.A.A. Applied Aerodynamics Conference, Albuquerque, NM, USA, June.

Nishino, T., 2007, Dynamics and Stability of Flow Past a Circular Cylinder in Ground Effect, Ph.D. Thesis, Faculty of Engineering, Science and Mathematics, University of Southampton, 145p.

Price, S.J., Summer, D., Smith, J.G., Leong, K. and Paidoussis, M.P., 2002, "Flow Vizualization around a Circular Cylinder near to a Plane Wall", Journal of Fluids ans Structures, Vol. 16, pp. 175-191.

Recicar, J.N., Alcântara Pereira, L.A. and Hirata, M.H., 2008, "Fluid Flow and Heat Transfer around an Oscillating Circular Cylinder using a Particle Method", 12th Brazilian Congress of Thermal Sciences and Engineering, Proceedings of ENCIT 2008, November 10-14, Belo Horizonte, Brazil.

Ricci, J.E.R., 2002, "Numerical Simulation of the Flow around a Body in the Vicinity of a Plane Using Vortex Method", Ph.D. Thesis, Mechanical Engineering Institute, UNIFEI, Itajubá, MG, Brazil (in Portuguese).

Roshko, A., Steinolfson, A. and Chattoorgoon, V., 1975, "Flow Forces on a Cylinder near a Wall or near Another Cylinder", Proceedings of the 2nd US Nation Conference on Wind Engineering Research, Fort Collins, Paper IV-15.

Sarpkaya, T., 1989, "Computational Methods with Vortices - The 1988 Freeman Scholar Lecture", Journal of Fluids Engineering, Vol. 111, pp. 5-52.

Sarpkaya, T., 1979, "Vortex-Induced Oscillations", ASME J. Appl. Mech., 46:241-258.

Shintani, M. and Akamatsu, T, 1994, "Investigation of Two Dimensional Discrete Vortex Method with Viscous Diffusion Model", Computational Fluid Dynamics Journal, Vol. 3, No. 2, pp. 237-254.

Taneda, S., 1965, "Experimental Investigation of Vortex Streets", Journal of the Physical Society of Japan, Vol. 20, pp. 1714-1721.

Williamson, C.H.K. and Govardhan, R., 2004, "Vortex Induced Vibrations", Annu. Rev. Fluid Mech., 36:413-455.

Zdravkovich, M.M., 2003, "Flow around Circular Cylinders" Vol. 2: Applications, Oxford University Press, Oxford, UK.

Zdravkovich, M.M., 1985a, "Observation of Vortex Shedding behind a Towed near a Wall", Flow Visualization III: Proceedings of the Third International Symposium on Flow Vizualization, ed. W.J. Yang, Hemisphere, Washington DC, pp. 423-427.

Zdravkovich, M.M., 1985b, "Forces on a Circular Cylinder near a Plane Wall", Applied Ocean Research, Vol. 7, pp. 197-201.

7. RESPONSIBILITY NOTICE

The authors are the only responsible for the printed material included in this paper.